

# Method for Efficient Identification of Similar Work Pieces for X-Ray Computed Tomography

Robert SCHMITT\*, Christian NIGGEMANN\*

\*Laboratory for Machine Tools and Production Engineering at RWTH Aachen University, Chair of Metrology and Quality Management, Steinbachstraße 19, D-52074 Aachen Germany, +49 241 80 20 283, [r.schmitt@wzl.rwth-aachen.de](mailto:r.schmitt@wzl.rwth-aachen.de), +49 241 80 28 393, [c.niggemann@wzl.rwth-aachen.de](mailto:c.niggemann@wzl.rwth-aachen.de)

**Abstract.** For metrological X-Ray Computed Tomography it is preferable that well established values for imaging parameters such as tube voltage or exposure time could be adapted to new parts. Also it is desirable that the process variation derived from elaborate experimental analyses for the estimation of the uncertainty in measurement could be transferred to similar cases. The guideline VDI/VDE 2630 permits this for sufficient similarity for boundary conditions, measurement strategy, size and material to a reference object. However, the similarity is not expressed in characteristics or even quantified so that an objective assessment could be made.

The proposed approach aims at the efficient and objective identification of similar work pieces to reduce the experimental effort to find adequate parameter sets for new parts. For this the similarity is categorized in shape, scale and material to assess the attenuation behaviour and the measurement task. Providing a part geometry and material composition the simulation calculates similarity characteristics, which then can be compared to those of reference parts.

The similarity of shape is assessed by means of 2D Fourier descriptors. The similarity of scale is based on local penetration lengths calculated by ray tracing. The similarity of material considers the composition and predicts the attenuation based on the Lambert-Beer-Law. The similarity is simulated for test piece and real part geometries using typical aluminium alloys, steel alloys and plastics.

## 1. Set-up of Industrial X-Ray Computed Tomography Measurements

Industrial X-Ray Computed tomography (CT) is increasingly used also for the measurement and quality assurance of geometric work piece features [1]. CT is a non-destructive imaging process, which is capable to acquire the work piece holistically with very high point density. The result of the tomographic scan is a volumetric model of the work piece, approximating the 3D geometry and local density of the real part. The volumetric model can be used for versatile inspection tasks. These are the inspection of material defects, control of assemblies and the dimensional measurement. The quality of the volumetric model is essentially influenced by the parameters of the tomographic scan, thus affecting the uncertainty of the subsequent geometric measurement. Before the tomographic scan the user has to define the actual parameter values adapted to the work piece. These parameters are basically the tube voltage and current, the thickness of the physical filter, the number of projections, the detector gain and the exposure time [2]. Due to this large number of parameters, the finding of this adequate parameter set-up can be

time consuming, e.g. doing experimental test series. The complexity of the tomographic imaging and the effects of the parameters onto the projection images make it difficult for the user to assess which set-up provides the smallest uncertainty. Also expert users may be misled or can take disadvantageous decisions for a new work piece. At any rate the user influence remains high for the set-up stage. So it is preferable that the knowledge gained by undertaken experimental effort in the past can be used to find the appropriate decision for a new part faster. The same applies to the knowledge from experimental studies to obtain the process variation  $u_p$  and the bias  $b$  to the calibrated value for the estimation of the uncertainty in measurement according to ISO/DIS 15530-3 [3] (Method using calibrated work pieces). In this context the question about the similarity of the actual to the reference work piece, for which the study has been made, occurs.

## 2. Similarity of Work Pieces

In order that it is permissible to adapt optimal parameter values derived from an expert study to a new work piece sufficient similarity between the two work pieces is mandatory. The concept of similarity is concern of various scientific fields of research.

For multi-variate statistics the similarity between to objects is defined by similarity of distance measures [4]. Usually for metric variables distance measures are used.

For geometry two figures are congruent when they can be matched by applying geometric transformation such as centric dilatation, shifting, rotation or reflection [5]. The geometry of work pieces is usually much more complex compared to basic geometries so that even for a slight change never an exact match would be possible.

The similitude theory describes the model of a physical process by dimensionless characteristics [6]. This theory is applied for theoretical analyses and experimental studies. Typical fields are fluid dynamics and heat transfer. In case that all relevant characteristics are equal between the process and the model of this process it is assured that both domains are physically similar. Results derived from the model, e.g. by simulation, can than be transferred to the physical process. The equality of the dimensionless characteristics requires also the geometric similarity between the reality and the model.

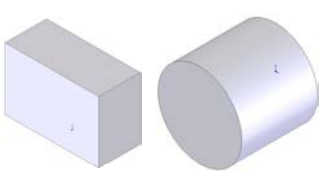
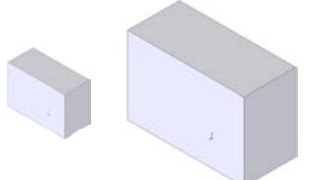
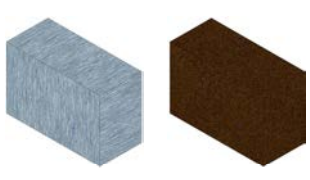
The similarity of shapes is intensively analysed for the computer graphics, e.g. for the scene recognition, object recognition, object tracing. For this various approaches exist, e.g. using Fourier descriptors (FD) [7, 8], Lightfield descriptors (LFD) [9] or distance measures [10].

Basically, ISO/DIS 15530-3 [3] requires that for standards and work pieces measures, angles, form deviation, surface structure, material (e.g. thermal expansion, elasticity, hardness) should be similar. Also for tactile coordinate metrology the measurement strategy (number and distribution of spatial points assigned to the measurement element) and the configuration of the probe have to be equal. For distances similarity is achieved when the work piece does not deviate more than 10 % from the reference ( $> 250$  mm) or more than 25 mm ( $< 250$  mm) respectively. Similarity for angles is assured within a range of  $\pm 5^\circ$  around the reference angle. Similarity for form and material are not quantified. In addition, the CT specific guideline VDI/VDE 2630-1.3 [11] requires similar attenuation properties (mass attenuation coefficient, density, porosity) so that material and geometry dependent factors onto the measurement are nearly the same for the actual and the reference work piece. Helpful for this are accomplished suitability tests for similar work pieces. However, the similarity is not quantified; making it difficult to decide if similarity is given or not.

### 3. Concept for the Efficient Identification of Similar Work Pieces

Before defining an adequate parameter set-up it is sensible to search for similar cases in the tomography database, e.g. for a work piece variant, to analyse if it is possible to adapt the parameter values to the actual case. This database is usually provided by the manufacturer of the CT system. It contains information about past tomographic scans, e.g. the user, the name of the work piece and the parameter set-up. Not yet included in the database are the geometric representation (CAD-model) and the material composition of the work piece.

For CT as necessary condition the similarity has to cover the shape, the size and the material of the work piece (Figure 1). The size of the work piece affects the penetration lengths of the X-Rays within the solid material, which directly affects the remaining intensity according to the exponential attenuation law. This influence also applies to the material composition. The shape of the work piece considers the spatial alignment of simpler regular geometries (macro geometry), which form the work piece. The effect of the shape onto the measurement is related to the size and the material distribution but also considers implicitly the effect of scattering radiation or artefacts. For instance, beam hardening artefacts in the voxel model often occur at work piece edges, which are usually disadvantageous regarding the uncertainty in measurement. Also the shape is correlated to the measurement element and the features respectively, e.g. if a diameter of a cylinder has to be measured or a distance between to parallel planes. In case of significant form deviations or high roughness (micro geometry) a fourth similarity domain could be added.

Shape	Scale	Material
		
Control var.: FD-distance measure $d(F_{1,i}, F_{2,i}) = \sum_{v=1}^V  F_{1,i,v} - F_{2,i,v} $	Control var.: Max. penetration length $MaxPL = \max \left\{ \sum_{w=1}^{Q/2} \left\  \vec{p}_{j,2w} - \vec{p}_{j,2w-1} \right\ _2 \right\}_{OA}$	Control var.: Lin. Attenuation coeff. $\mu_{Mat}(E) = \rho_{Mat} \cdot \sum_{i=1}^{92} w_i \cdot \left( \frac{\mu}{\rho} \right)_{E,Element.i}$
Test criterion: $d < d_{crit}$	Test criterion: $PL_{min} < MaxPL < PL_{max}$	Test criterion: $\mu_{min} < \mu_{Mat} < \mu_{max}$

**Figure 1.** Similarity Domains for X-Ray Computed Tomography

To assess the similarity of two work pieces, characteristics for the aforementioned similarity domains have to be derived and compared. For a non-ambiguous decision also a tolerance band for each characteristic is necessary. It is sensible to store the characteristics or the information from which the characteristic can be calculated for done tomographic scans in the database. For a similarity inquiry the stored values are read and then compared with the calculated values for the new part. Sufficient similarity between the actual part and the reference part is achieved when for all categories the characteristic values for the actual part are within the defined tolerance band around the reference values.

It is suggested to assess the similarity of shape by comparing the distance measure of LFD  $d$  of the actual part ( $F_1$ ) and the reference part ( $F_2$ ) (see 3.1). The test criterion is fulfilled when  $d < d_{crit}$ . For the similarity of scale the maximum penetration lengths for the optimal part orientation [12] are compared (see 3.2). The control variable has to be between the penetration length  $PL_{min}$  and  $PL_{max}$ . To prove the similarity of the material the linear attenuation coefficients for the actual material are compared to those for the reference

material for the photon energies of the emitted spectrum. For a sufficient similarity the linear attenuation coefficients have to be within a tolerance band around the reference curve. For similar penetration lengths and similar attenuation coefficients a similar intensity reduction can be expected. This leads to similar greyscale projection images, which are the base for the volumetric model, which itself is the base for the geometric measurement.

The suggested similarity analysis is in accordance with the major requirements of VDI/VDE 2630 Sheet 1.2. For the similarity of the measurement additionally to the basic similarity of the work piece also the same reconstruction and segmentation algorithm, the same registration of the point cloud and the same measurement strategy have to be applied.

### 3.1 Similarity of Shape

The similarity of shape is assessed by means of LFD, which are a special case of 2D FD. Fourier descriptors are utilised for the compact description of plane closed curves. The FDs represent the point cloud by a series of periodic functions. Originally these descriptors have been designed for the storage space optimized description of point clouds [13]. LFD use parallel projection to generate the plane curves [9]. The procedure to calculate the LFD from the geometric work piece representation is outlined in Figure 2.

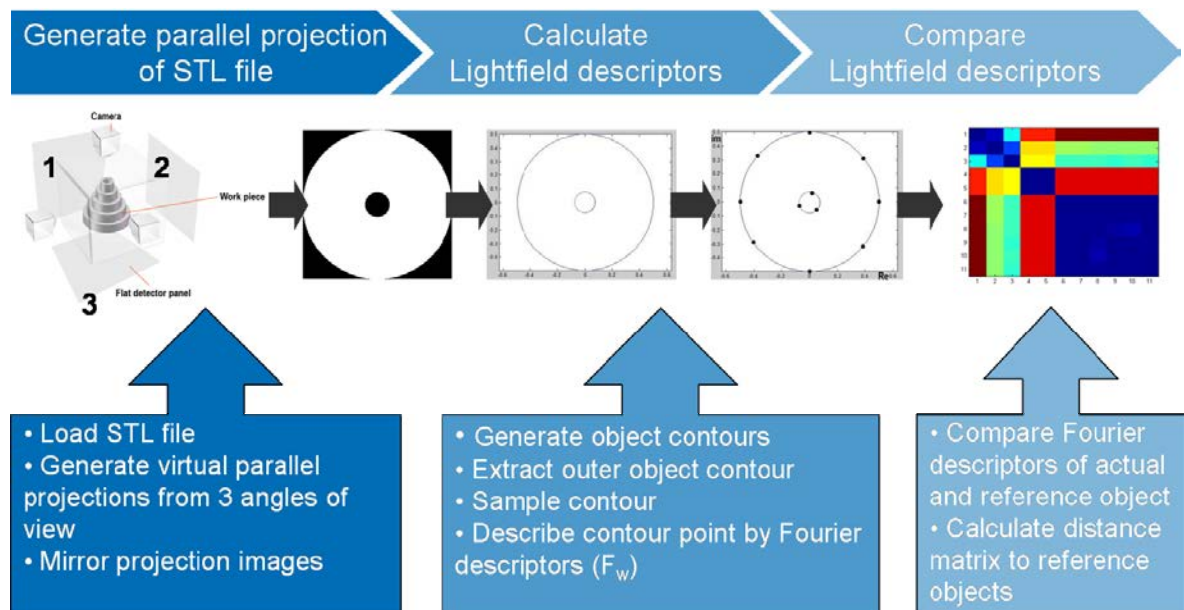


**Figure 2.** Procedure to assess the similarity of shape by means of Lightfield descriptors

The geometric work piece representation (STL file) is loaded. STL is a common CAD interface approximating the nominal geometry by triangular facets. From the STL file parallel projections are made from 3 angles of view returning binary images. The angles of view are located on the planes of the cubic bounding box surrounding the point cloud (facet model). Altogether 6 views are possible from a cuboid, whereas 2 opposite views return mirrored images. When the rays penetrate solid material the grey value is set to 1 while for the background the value is set to 0. From the binary images contour images are generated. The outer contour is extracted. Subsequently this contour is sampled by a discrete number of points. To each point a complex number  $x_n + i \cdot y_n$  is assigned, whereas the real part is the x-coordinate and the imaginary part is the y-coordinate in the image coordinate system. From these points the 2D Fourier descriptors can be calculated as follows:

$$F(w) = \frac{1}{N} \sum_{n=1}^{N-1} (x(n) + jy(n)) \cdot e^{(-j \cdot 2\pi wn / N)}$$

In the frequency domain the contour signal is concentrated on few descriptors only. Most absolute FD values for higher frequencies are small compared to the signal amplitude. By neglecting frequencies beyond the cut-off frequency the whole signal is not changed significantly. So the contour signal can be approximated quite well by only a few FD. These FD can be stored in the database. To assess the similarity  $D$  of two point clouds  $m_1$  and  $m_2$  first they have to be registered by best-fit. This is necessary because one point cloud can be a shifted or rotated version of the first one. The best-fit is achieved by gradual rotation of the actual point cloud towards the reference point cloud whereas the orientation is based on the planes of the cubic boundary box. For the optimal angular position of the work piece the distance measure of the two point clouds is the sum of the distances  $d$  of the  $I$  different  $F_{1,i}$  and  $F_{2,rot(i)}$ , which are the FD of the  $i$ -th projection image.

$$D(m_1, m_2) = \min_{rot} \sum_{i=1}^I d(F_{1,i}, F_{2,rot(i)})$$

Every projection image can have up to 3 FD. The distance measure is evaluated for the minimum distance between each contour of the  $i$ -th projection image as follows:

$$d(F_{1,i}, F_{2,i}) = \sum_{v=1}^V |F_{1,i,v} - F_{2,i,v}|$$

The Fourier descriptors of the actual work piece are compared to the respective values of the work pieces in the database, so that for each comparison a distance measure is given. From this a matrix can be formed containing the cross-linked distance measure. This distance matrix can be stored as txt-file or visualised as colour-coded distance map.

### 3.2 Similarity of Size

The similarity of scale is assessed comparing the maximum penetration length of the actual part and the reference part for the respective optimal alignment. The maximum penetration length is an essential indicator for the set-up of the tube voltage, which determines the hardness of the radiation. It has to be assured that the work piece is sufficiently penetrated even for the longest path length within solid material or for the path with the highest attenuation in case the local linear attenuation coefficients vary, e.g. for multi-material parts. The maximum penetration lengths are also stored in the database.

The local penetration lengths are calculated using a Matlab-based ray-tracing simulation [see also 12]. The facet model of the work piece is positioned in the simplified geometric model of the CT system (Figure 3). Necessary data are the Source-Detector-Distance (SDD) and the detector size. Then the facet model is inclined around the x-axis of the work piece coordinate system and rotated in a similar way compared to the real tomographic imaging process around the z-axis. It is sensible to incline the facet model gradually from  $0^\circ$  to  $90^\circ$ . The inclination is then redone for the y-axis of the work piece coordinate system. For each angle combination the penetration length is calculated for a discrete number of rays, which are aligned in a regular grid. In the middle of Figure 3 the penetration length map is visualised for two angles (inclination  $0^\circ$ , orientation  $90^\circ$  and  $90^\circ$ ,  $0^\circ$ ) at  $1024 \times 1024$  rays. The maximum penetration length for one inclination includes is the longest path length within the solid material for all defined rays and all rotation steps for that specific inclination. The optimum orientation is considered that specific orientation for which the maximum penetration length reaches a minimum. The predicted energy-dependent attenuation can then be calculated based on the penetration length map (Figure 3 right, examples for photon energy of 250 keV).

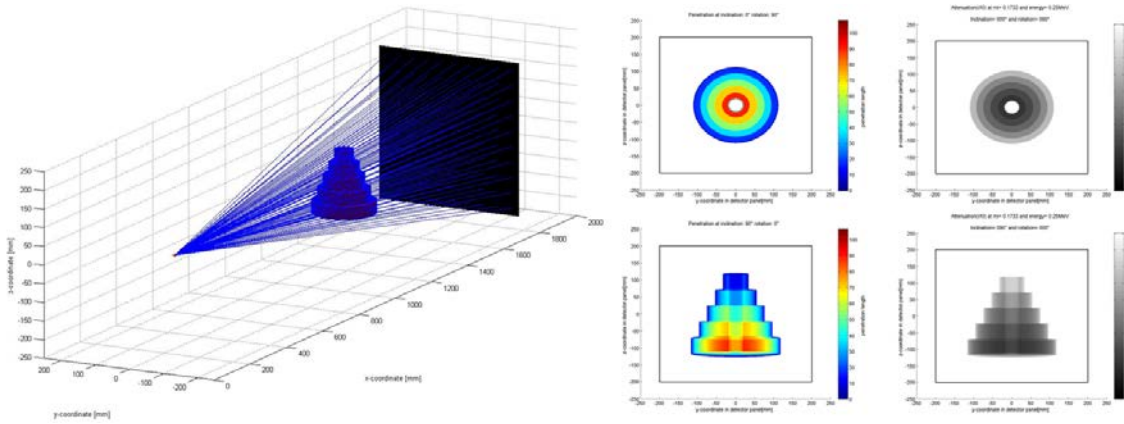


**Figure 3.** Visualisation of ray-tracing simulation and results as base for the similarity analysis

### 3.3 Similarity of Material

The matrices with the local penetration lengths available for each angle combination can be combined with the material and photon energy dependent linear attenuation coefficients. For this the linear attenuation coefficient vs. ray energy curve for the material is needed, which is a superposition of the curves of the involved chemical elements. The superposition is related to the mass percentage of each element, as it is assumed that each element contributes to the overall attenuation to the same extent as its mass percentage. The curve is calculated by summing up the weighted energy dependent mass attenuation coefficients [14]. For this superposition it is necessary to have the values at the same energies. This requires a refined energy array containing beside the tabulated node energies all attenuation edge energies. Intermediate values are interpolated using cubic splines, which range from one to the next attenuation edge. The linear attenuation coefficient vs. energy curve is then calculated by multiplying the mass attenuation values with the known material density. The weight percentage can be taken from standards, material databases or data sheets provided by the material provider. For given permissible ranges for the weight percentage, e.g. 15-17 %, the mean value 16 % is taken.

## 4. Results and Conclusions

In Figure 4 a similarity map is shown for various volume primitives such as step cylinders, cubic blocks with and without a bore hole and cylinders with and without a bore hole at different approximation qualities (“coarse” (Part No. 6, 9), “fine” (7, 10) and “Maximum resolution” (8, 11)). The approximation quality concerns the radial distance towards the nominal surface and the angle characterised by the chord. It is evident that the comparison between a facet model with itself leads to a distance measure of 0 meaning an identical shape. Also the distance map is symmetric, so it does matter if the actual geometry and the reference geometry are reversed. The results reveal that the approximation quality has only a little effect on the distance measure (< 20) while a significant effect is observed between round shaped parts and cubic parts. So a classification would be possible to distinguish box-like parts from rotation-symmetric parts, whereas the threshold is approximately at 500. Also it is observed that internal features as the bore hole are not changing the distance measure significantly. The reason for this is that for the comparison of contours the number of contours always has to match. So it is the outer contours of the binary projection images, which is decisive.

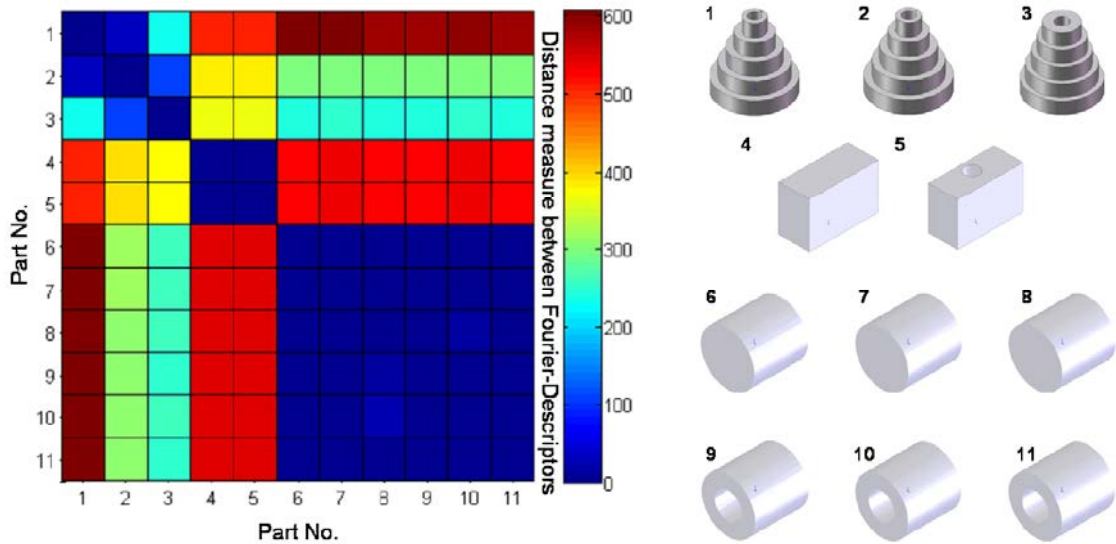


**Figure 4.** Similarity of Shape for volume primitives

The results of the penetration length simulation are shown below in Figure 5. Here for the step cylinder (Part No. 2) the maximum penetration length over all defined rays is plotted vs. the rotation and inclination angle (angular increment for rotation and inclination  $5^\circ$ ). On the left side the results are for the inclination around the x-axis of the work piece coordinate system while on the right side the results are for the inclination around the y-axis. The step cylinder is originally orientated horizontally as defined in the CAD model, while for an inclination of  $90^\circ$  around the x-axis the step cylinder is upright as illustrated in Figure 4. The step cylinder has a maximum diameter of 90 mm and a height of 90 mm.

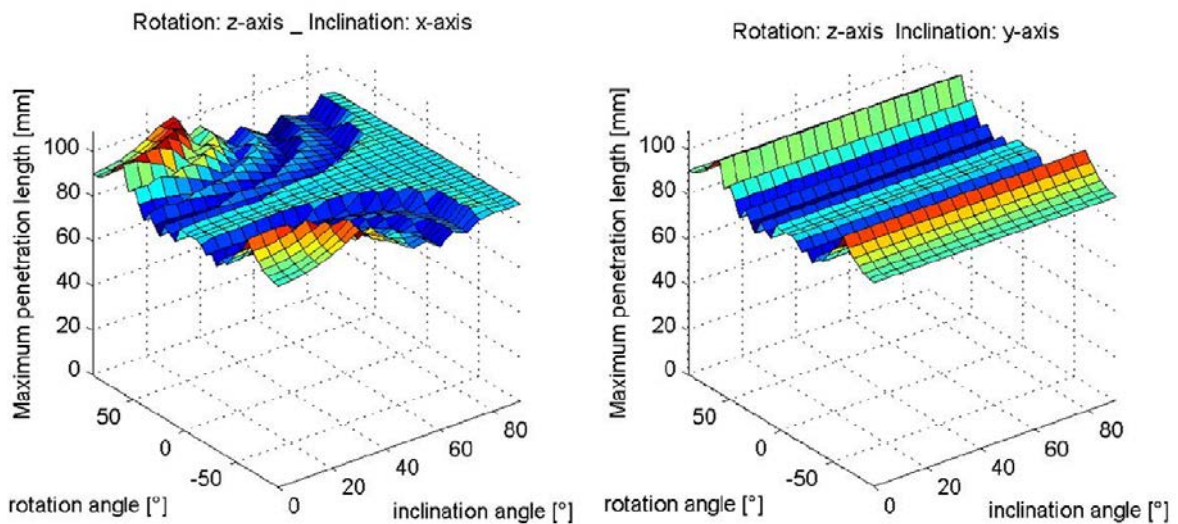


**Figure 5.** Maximum Penetration Length dependent on the work piece orientation for step cylinder

For the upright orientation ( $90^\circ$ ) the maximum penetration length remains almost unchanged as the step cylinder is rotation symmetric around the z-axis. For the inclination around the y-axis the inclination angle has no effect as the y-axis is the rotation axis of the step cylinder, so by changing the inclination angle the step cylinder only rotates around its own axis. But generally both inclination axes have to be considered to assure that the penetration length optimized orientation of the work piece can be found. For this case a disadvantageous orientation would be the horizontal one as for this higher maximum penetration length occurs. With the applied simulation the operator is able to find that

optimal inclination and can then compare the calculated penetration length with the value for the reference work piece. According to ISO/DIS 15530-3 a coarse estimation of the permissible range for the similarity of size would then be  $81.54 \pm 25$  mm.

In Figure 6 left for various standardized aluminium alloys [15] the relative deviation of the linear attenuation coefficient is shown respectively to the linear attenuation coefficient of pure aluminium. It can be observed that especially for lower photon energies higher deviations ( $\sim 10$ - $20$  %, partly up to  $110$  %) occur, while for photon energies near the maximum energy, which can be provided by common industrial CT systems ( $225$  keV- $450$  keV) the deviations fall below  $5$  %. One reason is the presence of attenuation edges, which are more numerous for alloys and have no correspondent edge in aluminium. The second reason is that in the alloy more absorbing elements are present, e.g. a higher content of copper (EN AW-2014) or zinc (EN AW-7003, EN AW-7475). For a penetration length of  $10$  cm in solid material (approximate value for the step cylinder (2) in Figure 4) the relative deviation for the Intensity reduction would be within a range of  $+6.47$  % (EN AW-5356) and  $-19.6$  % (EN AW-7475) for the photon energy of  $200$  keV and relative deviations of  $\mu$  of  $-19.0$  % and  $+6.59$  % respectively.

Similar evaluations have been done also for steel alloys and various precision plastics (Figure 6 right) using either a material composition database [16] or the molecular formula of the monomer. For latter the mass percentage is calculated from the element ratio and the molar mass. Plastics are a compound containing beside the polymer reinforcement materials such as fibres, ceramic powder or carbon also additional substances, whereas the exact mixture is the property of the compounder and therefore not disclosed. A spectroscopic measurement could improve the quality of the material representation used for the similarity analysis. For the plastics the reference has been POM. Here for PVC and PSU deviations occur up to  $800$  % due to more absorbing chlorine and sulphur nuclei.

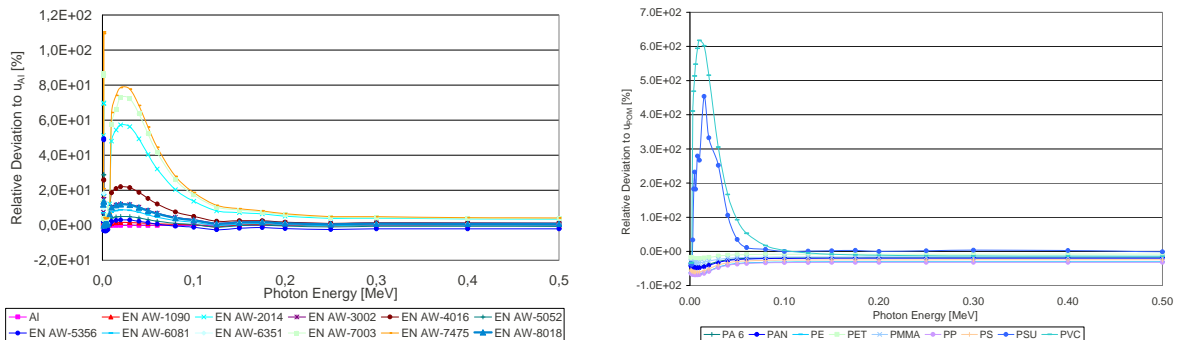


**Figure 6.** Similarity of Material (linear attenuation coefficient) for various aluminium alloys and plastics

Regarding the similarity analysis a thorough investigation has to reveal at which intensity deviation a significant change for the uncertainty of the measurement process  $u_p$  and the bias  $b$  occurs. Here we propose an experimental study using the same geometry but with different materials and a study with modular volume primitives, i.e. a geometry set-up by smaller entities, so that the geometry could be rearranged. This would lead to the values of the tolerance band introduced in Figure 1. A higher intensity reduction is seen more critical than the adaptation to a material, which is less absorbing. So the tolerance band will not be symmetrical towards the reference value.

## 5. Acknowledgements

This work is supported by the Deutsche Forschungsgemeinschaft DFG within the scope of the German-Brazilian Research Initiative BRAGECRIM (reference SCHM1856/13-1).



## References

- [1] Bartscher, M., Hilpert, U., Härtig, F., Neuschaefer-Rube, U., Goebbels, J., Staude, A., Industrial Computed Tomography, an emerging coordinate measurement technology with high potential, Proc. of NCSL International Workshop and Symposium, 2008.
- [2] VDI/VDE 2630 Sheet 1.2, Guideline, Computed tomography in dimensional measurement - Influencing variables on measurement results and recommendations for computed tomography dimensional measurements, 2010-11
- [3] ISO/DIS 15530-3, Standard Draft, Geometrical product specifications (GPS) - Coordinate measuring machines (CMM): Technique for determining the uncertainty of measurement - Part 3: Use of calibrated workpieces or standards, 2009-05
- [4] Härdle, W., Simar, Applied Multivariate Statistical Analysis. 1. Edition, Springer, Berlin 2003
- [5] Ross, D., Master Math: Geometry, Course Technology PTR Pub, ISBN-10: 1-59863-986-2, 2009
- [6] Kline, S., Similitude and Approximation Theory, Springer, New York, 1986
- [7] Zahn, C.T., Roskies, R.Z., 1972, Fourier Descriptors for Plane Closed Curves, EE Transactions on Computers, Vol. c-21: 269–281
- [8] Zhang, D., Lu, G., 2001, Content-Based Shape Retrieval Using Different Shape Descriptors: A Comparative Study, IEEE International Conference on Multimedia and Expo: 1139–1142
- [9] Chen, D.Y., Tian, X.P., Shen, Y.-T., Ouhyoung, M., 2003, On Visual Similarity Based 3D Model Retrieval, Eurographics: 223–232
- [10] Schmitt, R., Fritz, P.: Intelligent Descriptor Models for Automated Engineering Shape Classification in Quality Control. Proceedings of CIRP ICME, 23 - 25 June 2010, Capri, Italy
- [11] VDI/VDE 2630 Sheet 1.3, Guideline Draft: Computed tomography in dimensional measurement; Guideline for the application of DIN EN ISO 10360 for coordinate measuring machines with CT-sensors, 2009-08
- [12] Schmitt, R., Niggemann, C.: Einfluss der Bauteilorientierung auf die Messunsicherheit bei dimensionellen Computertomografie Messungen in: Industrielle Computertomografie Tagung 2010 - Proceedings, Hrsg.: Kastner, J., 1. Aufl., Shaker, Aachen, 221-226
- [13] Schmitt, R., Fritz, P.: A 3D-Fourier-Descriptor Approach to Compress 3D Imaging Data in: Sensor+Test Conference 2009 Proceedings OPTO 2009, 133-138
- [14] <http://physics.nist.gov/PhysRefData/XrayMassCoef/tab3.html>
- [15] DIN EN 573-3: Aluminium and aluminium alloys - Chemical composition and form of wrought products - Part 3: Chemical composition and form of products; German version EN 573-3:2009
- [16] <http://www.stahlschluessel.de/en/home.html>